# CLF-based Tracking Control for UAV Kinematic Models with Saturation Constraints

Wei Ren     Randal W. Beard
Department of Electrical and Computer Engineering
Brigham Young University
Provo, Utah 84602

*Abstract*— **This paper considers the trajectory tracking problem for unmanned air vehicles (UAVs). We assume that the UAV is equipped with an autopilot which reduces the twelve degree-of-freedom (DOF) model to a six DOF model with altitude, heading, and velocity command inputs. In this paper we restrict our attention to planar motion. One of the novel features of our approach is that we explicitly account for heading and velocity input constraints. For a fixed wing UAV, the velocity is constrained to lie between two positive constants, and therefore presents particular challenges for the control design. We propose a control Lyapunov function (CLF) approach. We first introduce a CLF for the input constrained case, and then construct the set of all constrained inputs that render the CLF negative. The control input is then selected from this "feasible" set. The proposed approach is then applied to a simulation scenario, where a UAV is assigned to transition through several targets in the presence of multiple dynamic threats.**

## I. INTRODUCTION

The stabilization and tracking of dynamical systems with nonholonomic constraints has received recent attention in the literature. An inherent challenge, identified by Brockett's well-known necessary condition for feedback stabilization [1], is that nonholonomic systems cannot be stabilized via smooth time-invariant state feedback. A simple but classical example of a nonholonomic system is a mobile robot which serves as an interesting topic for stabilization and tracking (c.f. [2], [3], [4]). Unmanned air vehicles (UAVs) equipped with low-level altitude-hold, velocity-hold, and heading-hold autopilots can be modeled by kinematic equations of motion that are similar to the kinematic equations of motion of mobile robots. However, while mobile robots and UAVs have similar angular velocity, or heading rate, constraints, the linear velocity constraints are quite different. In particular, fixed wing UAVs have a minimum velocity constraint that is greater than zero, due to the stall conditions of the aircraft, while mobile robots may have negative linear velocity. As a result, existing approaches for mobile robots are not directly applicable to fixed wing UAVs since negative velocities are allowed. This paper deals with the issue of tracking control for UAV kinematic models with physically motivated heading rate and velocity constraints. We approach the problem using control Lyapunov functions (CLFs) [5], [6]. While our approach is designed for UAVs in particular, it is also valid for mobile robot kinematic models with similar input constraints.

In this paper, we take the following approach to UAV trajectory tracking. We first propose a time-varying, constrained CLF for the UAV kinematic model. Following [7], the CLF is used to define a state-dependent, time-varying set of "feasible" control values from which different controllers can be instantiated. Selection from this feasible control set, guarantees accurate tracking as well as satisfaction of the saturation constraints. As noted in [7], different control strategies can be derived by selection from the feasible control set according to some auxiliary performance index. This approach introduces a great deal of flexibility to the tracking control problem. In this paper we propose a simple selection scheme based on saturation functions. The motivation for this selection scheme is computational simplicity. It is worthwhile to mention that the existing CLF based universal formulas are not feasible in the UAV case due to the velocity constraints.

The salient features of our approach are as follows. First, under the proposed tracking CLF framework with input constraints, we allow the reference velocity and angular velocity to be piecewise continuous while other approaches to tracking control (e.g. [3], [4]) constrain them to be uniformly continuous in order to apply Barbalat's lemma. Second, using different selection schemes, our approach can be used to derive a variety of other trajectory tracking strategies. Finally, it is computationally simple and can be implemented on off-the-shelf inexpensive microcontrollers. To illustrate the effectiveness of the controller, we apply our approach to a UAV scenario, where the UAV is assigned to transition through several opportunities in the presence of dynamic hazards. Instead of following simple paths composed of straight lines and circles (e.g. [3], [4]), the UAV tracks a trajectory generated dynamically from the trajectory generator described in [8], which responds the current, possibly time-varying, opportunity/hazard scenario presented to the UAV.

## II. PROBLEM STATEMENT

Following [9], we assume that each UAV is equipped with standard autopilots for heading hold and Mach hold. In order to focus on the essential issues, we will assume that altitude is held constant. Let $(x, y)$, $\psi$, and $v$ denote the inertial position, heading angle, and velocity for the UAV respectively. Then the resulting kinematic equations of motion are

$$
\begin{aligned}
\dot{x} &= v\cos(\psi) \\
\dot{y} &= v\sin(\psi) \\
\dot{\psi} &= \alpha_\psi(\psi^c - \psi) \\
\dot{v} &= \alpha_v(v^c - v),
\end{aligned}
\tag{1}
$$

where $\psi^c$ and $v^c$ are the commanded heading angle and velocity to the autopilots, and $\alpha_\psi$ and $\alpha_v$ are positive constants [9]. In addition, we assume that each UAV has the constraints that $v_{min} \leq v \leq v_{max}$ and $-\omega_{max} \leq \dot{\psi} \leq \omega_{max}$, where $v_{min} > 0$ and $\omega_{max} > 0$ is the saturated heading rate.

Assuming that $\alpha_v$ is large compared to $\alpha_\psi$, Eq. (1) reduces to

$$
\begin{aligned}
\dot{x} &= v^c \cos(\psi) \\
\dot{y} &= v^c \sin(\psi) \\
\dot{\psi} &= \alpha_\psi(\psi^c - \psi).
\end{aligned} \tag{2}
$$

Letting $\psi^c = \psi + \frac{1}{\alpha_\psi}\omega^c$, Eq. (2) becomes

$$
\begin{aligned}
\dot{x} &= v^c \cos(\psi) \\
\dot{y} &= v^c \sin(\psi) \\
\dot{\psi} &= \omega^c
\end{aligned} \tag{3}
$$

with input constraints that $v_{min} \leq v^c \leq v_{max}$ and $-\omega_{max} \leq \omega^c \leq \omega_{max}$. Note that if $v_{min} = -v_{max}$, then Eq. (3) is the same as the kinematic model for a mobile robot with similar input constraints.

In this paper we will assume the existence of a reference trajectory $(x_r, y_r, \psi_r, v_r, \omega_r)$ which satisfies

$$
\begin{aligned}
\dot{x}_r &= v_r \cos(\psi_r) \\
\dot{y}_r &= v_r \sin(\psi_r) \\
\dot{\psi}_r &= \omega_r
\end{aligned} \tag{4}
$$

under the constraints that $v_r$ and $\omega_r$ are piecewise continuous and satisfy the constraints $v_{min} + \epsilon_v \leq v_r \leq v_{max} - \epsilon_v$ and $-\omega_{max} + \epsilon_\omega \leq \omega_r \leq \omega_{max} - \epsilon_\omega$, where $\epsilon_v$ and $\epsilon_\omega$ are positive constants. The inclusion of $\epsilon_*$ in the constraints of the reference trajectory generator, guarantees that there is sufficient control authority to track the trajectory. We will see that as $\epsilon_*$ approach zero, the feasible control set vanishes. The control objective is to find feasible control inputs $v^c$ and $\omega^c$ such that $|x_r - x| + |y_r - y| + |\psi_r - \psi| \to 0$ as $t \to \infty$.

Transforming the tracking errors expressed in the inertial frame to the UAV frame, the error coordinates [10] can be denoted as

$$
\begin{bmatrix} x_e \\ y_e \\ \psi_e \end{bmatrix} = \begin{bmatrix} \cos(\psi) & \sin(\psi) & 0 \\ -\sin(\psi) & \cos(\psi) & 0 \\ 0 & 0 & 1 \end{bmatrix} \begin{bmatrix} x_r - x \\ y_r - y \\ \psi_r - \psi \end{bmatrix}. \tag{5}
$$

Accordingly, the tracking error model can be represented as

$$
\begin{aligned}
\dot{x}_e &= \omega^c y_e - v^c + v_r \cos(\psi_e) \\
\dot{y}_e &= -\omega^c x_e + v_r \sin(\psi_e) \\
\dot{\psi}_e &= \omega_r - \omega^c.
\end{aligned} \tag{6}
$$

Following [4], Eq. (6) can be simplified as

$$
\begin{aligned}
\dot{x}_0 &= u_0 \\
\dot{x}_1 &= (\omega_r - u_0)x_2 + v_r \sin(x_0) \\
\dot{x}_2 &= -(\omega_r - u_0)x_1 + u_1,
\end{aligned} \tag{7}
$$

where

$$
(x_0, x_1, x_2) = (\psi_e, y_e, -x_e) \tag{8}
$$

and $u_0 \triangleq \omega_r - \omega^c$ and $u_1 \triangleq v^c - v_r \cos(x_0)$.

The input constraints under the transformation become

$$
-\epsilon_\omega \leq u_0 \leq \epsilon_\omega \qquad \underline{v} \leq u_1 \leq \bar{v}, \tag{9}
$$

where $\underline{v} \triangleq v_{min} - v_r \cos(x_0)$ and $\bar{v} \triangleq v_{max} - v_r \cos(x_0)$. It is also easy to see that $v_{min} - v_{max} + \epsilon_v \leq \underline{v} \leq v_{min} + v_{max} - \epsilon_v$ and $\epsilon_v \leq \bar{v} \leq 2v_{max} - \epsilon_v$.

Obviously, Eqs. (5) and (8) are invertible transformations, which means $(x_0, x_1, x_2) = (0, 0, 0)$ is equivalent to $(x_e, y_e, \psi_e) = (0, 0, 0)$ and $(x_r, y_r, \psi_r) = (x, y, \psi)$. Therefore, the original tracking control objective is converted to a stabilization objective, that is, our goal is to find feasible control inputs $u_0$ and $u_1$ to stabilize $x_0$, $x_1$, and $x_2$.

Note from Eq. (7) that when both $x_0$ and $x_2$ go to zero, that $x_1$ becomes uncontrollable. To avoid this situation we introduce another change of variables.

Let $\bar{x}_0 = mx_0 + \frac{x_1}{\pi_1}$, where $m > 0$ and $\pi_1 \triangleq \sqrt{x_1^2 + x_2^2 + 1}$. Accordingly, $x_0 = \frac{\bar{x}_0}{m} - \frac{x_1}{m\pi_1}$. Obviously, $(\bar{x}_0, x_1, x_2) = (0, 0, 0)$ is equivalent to $(x_0, x_1, x_2) = (0, 0, 0)$. Therefore it is sufficient to find control inputs $u_0$ and $u_1$ to stabilize $\bar{x}_0$, $x_1$, and $x_2$. With the same input constraints (9), Eq. (7) can be rewritten as

$$
\begin{aligned}
\dot{\bar{x}}_0 &= (m - \frac{x_2}{\pi_1})u_0 + \frac{x_2}{\pi_1}\omega_r \\
&\quad + \frac{1+x_2^2}{\pi_1^3}v_r \sin\left(\frac{\bar{x}_0}{m} - \frac{x_1}{m\pi_1}\right) - \frac{x_1 x_2}{\pi_1^3}u_1 \\
\dot{x}_1 &= (\omega_r - u_0)x_2 + v_r \sin\left(\frac{\bar{x}_0}{m} - \frac{x_1}{m\pi_1}\right) \\
\dot{x}_2 &= -(\omega_r - u_0)x_1 + u_1.
\end{aligned} \tag{10}
$$

## III. CLF FOR TRACKING CONTROL WITH SATURATION CONSTRAINTS

In this section, we find a valid CLF for UAV trajectory tracking with input constraints. Consider the following class of affine nonlinear time-varying systems

$$
\dot{x} = f(t, x) + g(t, x)u, \tag{11}
$$

where $x \in \mathbb{R}^n$, $u \in \mathbb{R}^m$, and $f : \mathbb{R}_+ \times \mathbb{R}^n \to \mathbb{R}^n$ and $g : \mathbb{R}_+ \times \mathbb{R}^n \to \mathbb{R}^{n \times m}$ are locally Lipschitz in $x$ and piecewise continuous in $t$.

*Definition 1:* A continuously differentiable function $V : \mathbb{R}_+ \times \mathbb{R}^n \to \mathbb{R}$ is a control Lyapunov function (CLF) for system (11) with input constraints $u \in \mathcal{U} \subset \mathbb{R}^m$ if it is positive-definite, decrescent, radially unbounded in $x$, and satisfies

$$
\inf_{u \in \mathcal{U}} \left\{ \frac{\partial V}{\partial t} + \frac{\partial V}{\partial x}(f(t, x) + g(t, x)u) \right\} \leq -W_3(x), \tag{12}
$$

$\forall x \neq 0$ and $\forall t \geq 0$ where $W_3(x)$ is a continuous positive-definite function.

In order to find a CLF with bounded input constraints, we prefer the partial derivative of $V$ to be bounded. Accordingly, we have the following lemma.

*Lemma 2:* If $W(x) = \sqrt{x^T x + 1} - 1$, then $W(x)$ is continuously differentiable, radially unbounded, positive-definite, and $\left\| \frac{\partial W}{\partial x} \right\| \leq 1$.

*Proof:* Trivial. ∎

Lemma 2 will be used to construct a CLF for system (10). The following lemma defines a continuous positive-definite function.

*Lemma 3:* Let

$$
W_3(x) = \gamma_0 \left( \frac{\bar{x}_0}{\pi_2} \right)^2 + \gamma_1 k_1 \left( v_{\min} + \epsilon_v \right) \frac{x_1}{\pi_1} \sin \left( \frac{x_1}{m\pi_1} \right)
$$
$$
+ \gamma_2 \left( k_1 - \frac{1}{2} \right) \left( \frac{x_2}{\pi_1} \right)^2 \left( (v_{\min} + \epsilon_v) \cos \left( \frac{x_1}{m\pi_1} \right) - v_{\min} \right),
$$
(13)

where $\pi_2 \triangleq \sqrt{\bar{x}_0^2 + 1}$. If $k_1 > \frac{1}{2}$, $\gamma_i > 0$, and $m > 2/\cos^{-1}\left( \frac{v_{\min}}{v_{\min} + \epsilon_v} \right)$, then $W_3(x)$ is continuous and positive-definite.

*Proof:* Since $W_3$ is a composition of continuous functions, it is continuous. The first term in Eq. (13) is clearly positive and zero if and only if $\bar{x}_0 = 0$. The second term in Eq. (13) is nonnegative if $\left| \frac{x_1}{m\pi_1} \right| < \pi$. But since

$$
\left| \frac{x_1}{m\pi_1} \right| < \frac{1}{m} < \cos^{-1} \left( \frac{v_{\min}}{v_{\min} + \epsilon_v} \right) / 2 < \pi/4, \quad (14)
$$

the second term is positive and zero if and only if $x_1 = 0$. Since

$$
\left| \frac{x_1}{m\pi_1} \right| < \cos^{-1} \left( \frac{v_{\min}}{v_{\min} + \epsilon_v} \right) / 2 < \cos^{-1} \left( \frac{v_{\min}}{v_{\min} + \epsilon_v} \right)
$$
$$
\Longrightarrow \cos \left( \frac{x_1}{m\pi_1} \right) > \frac{v_{\min}}{v_{\min} + \epsilon_v}
$$
$$
\Longleftrightarrow (v_{\min} + \epsilon_v) \cos \left( \frac{x_1}{m\pi_1} \right) - v_{\min} > 0, \quad (15)
$$

the third term in Eq. (13) is positive and zero if and only if $x_2 = 0$. ∎

The following theorem defines a valid CLF for UAV trajectory tracking with input constraints.

*Theorem 4:* The function

$$
V = W(\bar{x}_0) + k_1 W \begin{pmatrix} x_1 \\ x_2 \end{pmatrix}
$$
$$
= \sqrt{\bar{x}_0^2 + 1} + k_1 \sqrt{x_1^2 + x_2^2 + 1} - (1 + k_1)
$$

is a CLF for system (10) with input constraints (9) if $W_3(x)$ is given by Lemma 3, $0 < \gamma_1 < 1$, $0 < \gamma_2 < 1$ and $m >$

$\max \left\{ M_0, 1 + \frac{d_2}{\epsilon_\omega} \right\}$, where

$$
M_0 \triangleq \max \left\{ \frac{2}{\cos^{-1}\left( \frac{v_{\min}}{v_{\min} + \epsilon_v} \right)}, 1 + \sqrt{2} \frac{d_1}{\epsilon_\omega} \right\} \quad (16)
$$

$$
d_1 \triangleq \left( k_1 + \frac{1}{2} \right) [2v_{\max} - \epsilon_v] + \gamma_2 (k_1 - \frac{1}{2}) \epsilon_v
$$
$$
+ k_1 \left[ (v_{\max} - \epsilon_v) + \gamma_1 (v_{\min} + \epsilon_v) \right]
$$
$$
+ (\omega_{\max} - \epsilon_\omega) + (v_{\max} - \epsilon_v) + \gamma_0 \quad (17)
$$

$$
d_2 \triangleq (v_{\max} - \epsilon_v)[\sqrt{2}(k_1 - \frac{1}{2}) \frac{M_2}{M_0} + \sqrt{2} k_1 \frac{M_1}{M_0} + 1]
$$
$$
+ (\omega_{\max} - \epsilon_\omega) + \gamma_0 \quad (18)
$$

and

$$
M_1 \triangleq \sup_{\substack{0 < |\alpha| < 1/M_0 \\ |\beta| < 1/M_0}} \left| \frac{\sin(\alpha - \beta) + \sin(\beta)}{\alpha} \right| \quad (19)
$$

$$
M_2 \triangleq \sup_{\substack{0 < |\alpha| < 1/M_0 \\ |\beta| < 1/M_0}} \left| \frac{\cos(\beta) - \cos(\alpha - \beta)}{\alpha} \right|. \quad (20)
$$

*Proof:* Obviously $V$ is positive-definite, decrescent, and radially unbounded, therefore it remains to show that $\dot{V} + W_3 \leq 0$, $\forall x \neq 0$.

Differentiating $V$ and setting $u_0 = -\epsilon_\omega \text{sign}(\bar{x}_0)$, we obtain the following expression after some algebraic manipulation:

$$
\dot{V} + W_3 = -\epsilon_\omega \frac{|\bar{x}_0|}{\pi_2} (m - \frac{x_2}{\pi_1}) + \sigma_1 u_1 + \sigma_2 + \sigma_3 + \sigma_4 \quad (21)
$$

where

$$
\sigma_1 = \left( k_1 - \frac{\bar{x}_0 x_1}{\pi_2 \pi_1^2} \right) \left( \frac{x_2}{\pi_1} \right)
$$

$$
\sigma_2 = \gamma_2 (k_1 - \frac{1}{2}) \left( \frac{x_2}{\pi_1} \right)^2 \left[ (v_{\min} + \epsilon_v) \cos \left( \frac{x_1}{m\pi_1} \right) - v_{\min} \right]
$$

$$
\sigma_3 = k_1 \left( \frac{x_1}{\pi_1} \right) \left[ v_r \sin(\frac{\bar{x}_0}{m} - \frac{x_1}{m\pi_1}) + \gamma_1 (v_{\min} + \epsilon_v) \sin \left( \frac{x_1}{m\pi_1} \right) \right]
$$

$$
\sigma_4 = \left( \frac{\bar{x}_0}{\pi_2} \right) \left[ \frac{x_2}{\pi_1} \omega_r + \frac{1 + x_2^2}{\pi_1^3} v_r \sin(\frac{\bar{x}_0}{m} - \frac{x_1}{m\pi_1}) + \gamma_0 \left( \frac{\bar{x}_0}{\pi_2} \right) \right].
$$

Three cases will be considered with respect to $\bar{x}_0$.

**Case 1:** $|\bar{x}_0| \geq 1$.
Since $|\bar{x}_0/\pi_2| < 1$, $|x_1/\pi_1^2| < 1/2$, and $|x_2/\pi_1| < 1$, we know that $|\sigma_1| \leq (k_1 + 1/2)$. Note that $\sigma_1 u_1 \leq (k_1 + 1/2)(2v_{\max} - \epsilon_v)$, $\sigma_2 \leq \gamma_2(k_1 - 1/2)\epsilon_v$, $\sigma_3 \leq k_1 [(v_{\max} - \epsilon_v) + \gamma_1(v_{\min} + \epsilon_v)]$, and $\sigma_4 \leq (\omega_{\max} - \epsilon_\omega) + (v_{\max} - \epsilon_v) + \gamma_0$. Since $m > 1 + \sqrt{2} d_1/\epsilon_\omega$, we get that $\dot{V} + W_3 \leq -\epsilon_\omega \frac{|\bar{x}_0|}{\pi_2}(m - 1) + d_1 \leq -\frac{\epsilon_\omega}{\sqrt{2}}(m - 1) + d_1 < 0$, where the second inequality comes from $|\bar{x}_0|/\pi_2 \geq 1/\sqrt{2}$ since $|\bar{x}_0| \geq 1$.

**Case 2:** $0 < |\bar{x}_0| < 1$.
Eq. (21) can be arranged as $\dot{V} + W_3 = \frac{|\bar{x}_0|}{\pi_2} \left\{ -\epsilon_\omega (m - \frac{x_2}{\pi_1}) + \frac{\pi_2}{|\bar{x}_0|} [\sigma_1 u_1 + \sigma_2 + \sigma_3 + \sigma_4] \right\}$. We will show that $d_2 \geq \frac{\pi_2}{|\bar{x}_0|}(\sigma_1 u_1 + \sigma_2) + \frac{\pi_2}{|\bar{x}_0|}\sigma_3 + \frac{\pi_2}{|\bar{x}_0|}\sigma_4$,

which implies that $m > 1 + d_2/\epsilon_\omega$ guarantees that $\dot{V} + W_3 \leq 0$.

Set $u_1 = v_{\min} - v_r \cos(\frac{\bar{x}_0}{m} - \frac{x_1}{m\pi_1})$ when $x_2 \geq 0$ and $u_1 = v_{\max} - v_r \cos(\frac{\bar{x}_0}{m} - \frac{x_1}{m\pi_1})$ when $x_2 < 0$.

In the case of $x_2 \geq 0$, noting that $(x_2/\pi_1)^2 \leq |x_2|/\pi_1$, $\left|\frac{\bar{x}_0}{m} - \frac{x_1}{m\pi_1}\right| < 2/m < \cos^{-1}(\frac{v_{\min}}{v_{\min}+\epsilon_v})$, $\left|\frac{\bar{x}_0 x_1}{\pi_2 \pi_1^2}\right| < \frac{1}{2}$, and $\cos\left(\frac{x_1}{m\pi_1}\right) > 0$, we get that

$$\frac{\pi_2}{|\bar{x}_0|}(\sigma_1 u_1 + \sigma_2)$$
$$= \frac{\pi_2}{|\bar{x}_0|}\{(k_1 - \frac{\bar{x}_0 x_1}{\pi_2 \pi_1^2})\left(\frac{|x_2|}{\pi_1}\right)\left[v_{\min} - v_r \cos\left(\frac{\bar{x}_0}{m} - \frac{x_1}{m\pi_1}\right)\right]$$
$$+ \gamma_2(k_1 - 1/2)\left(\frac{x_2}{\pi_1}\right)^2 [(v_{\min} + \epsilon_v)\cos\left(\frac{x_1}{m\pi_1}\right) - v_{\min}]\}$$
$$\leq \frac{\pi_2}{|\bar{x}_0|}\{(k_1 - 1/2)\left(\frac{|x_2|}{\pi_1}\right)\left[v_{\min} - v_r \cos\left(\frac{\bar{x}_0}{m} - \frac{x_1}{m\pi_1}\right)\right]$$
$$+ (k_1 - 1/2)\left(\frac{|x_2|}{\pi_1}\right)[v_r \cos\left(\frac{x_1}{m\pi_1}\right) - v_{\min}]\}$$
$$\leq \pi_2(k_1 - \frac{1}{2})v_r \frac{1}{m}\left|\frac{\cos\left(\frac{x_1}{m\pi_1}\right) - \cos\left(\frac{\bar{x}_0}{m} - \frac{x_1}{m\pi_1}\right)}{|\bar{x}_0|/m}\right|$$
$$\leq \sqrt{2}(k_1 - 1/2)(v_{max} - \epsilon_v)\frac{1}{M_0}M_2,$$

where the last inequality comes from $1/m < 1/M_0$, $\pi_2 < \sqrt{2}$ since $0 < |\bar{x}_0| < 1$, and Eq. (20) by letting $\alpha = \bar{x}_0/m$ and $\beta = x_1/(m\pi_1)$.

In the case of $x_2 < 0$, noting that $v_{max} - v_r \cos\left(\frac{\bar{x}_0}{m} - \frac{x_1}{m\pi_1}\right) \geq \epsilon_v$ and $(v_{min} + \epsilon_v)\cos\left(\frac{x_1}{m\pi_1}\right) - v_{min} \leq \epsilon_v$ we get that

$$\frac{\pi_2}{|\bar{x}_0|}(\sigma_1 u_1 + \sigma_2)$$
$$= \frac{\pi_2}{|\bar{x}_0|}\{(k_1 - \frac{\bar{x}_0 x_1}{\pi_2 \pi_1^2})\left(-\frac{|x_2|}{\pi_1}\right)\left[v_{\max} - v_r \cos\left(\frac{\bar{x}_0}{m} - \frac{x_1}{m\pi_1}\right)\right]$$
$$+ \gamma_2(k_1 - 1/2)\left(\frac{x_2}{\pi_1}\right)^2 [(v_{\min} + \epsilon_v)\cos\left(\frac{x_1}{m\pi_1}\right) - v_{\min}]\}$$
$$\leq \frac{\pi_2}{|\bar{x}_0|}\{(k_1 - \frac{1}{2})\left(-\frac{|x_2|}{\pi_1}\right)\epsilon_v + \gamma_2(k_1 - \frac{1}{2})\left(\frac{|x_2|}{\pi_1}\right)\epsilon_v\} \leq 0.$$

Note that

$$\frac{\pi_2}{|\bar{x}_0|}\sigma_3 \leq \frac{\pi_2}{|\bar{x}_0|}k_1 v_r \left(\frac{x_1}{\pi_1}\right)\left[\sin\left(\frac{\bar{x}_0}{m} - \frac{x_1}{m\pi_1}\right) + \sin\left(\frac{x_1}{m\pi_1}\right)\right]$$
$$\leq \pi_2 k_1 v_r \left|\frac{x_1}{\pi_1}\right|\frac{1}{m}\left|\frac{\sin\left(\frac{\bar{x}_0}{m} - \frac{x_1}{m\pi_1}\right) + \sin\left(\frac{x_1}{m\pi_1}\right)}{|\bar{x}_0|/m}\right|$$
$$\leq \sqrt{2}k_1(v_{\max} - \epsilon_v)\frac{1}{M_0}M_1,$$

where the first inequality comes from $\frac{x_1}{\pi_1}\sin\left(\frac{x_1}{m\pi_1}\right) \geq 0$ according to (14), and the last inequality comes from $\pi_2 <$

$\sqrt{2}$, $1/m < 1/M_0$, and Eq. (19) by letting $\alpha = \bar{x}_0/m$ and $\beta = x_1/(m\pi_1)$.

Also note that

$$\frac{\pi_2}{|\bar{x}_0|}\sigma_4$$
$$= \frac{\pi_2}{|\bar{x}_0|}\frac{\bar{x}_0}{\pi_2}\left[\frac{x_2}{\pi_2}\omega_r + \frac{1 + x_2^2}{\pi_1^3}v_r \sin\left(\frac{\bar{x}_0}{m} - \frac{x_1}{m\pi_1}\right) + \gamma_0\frac{\bar{x}_0}{\pi_2}\right]$$
$$\leq \left|\frac{x_2}{\pi_1}\omega_r\right| + \left|\frac{1 + x_2^2}{\pi_1^3}v_r \sin\left(\frac{\bar{x}_0}{m} - \frac{x_1}{m\pi_1}\right)\right| + \gamma_0\left|\frac{\bar{x}_0}{\pi_2}\right|$$
$$\leq (\omega_{\max} - \epsilon_\omega) + (v_{\max} - \epsilon_v) + \gamma_0.$$

Combining these expressions gives the desired result.

**Case 3:** $\bar{x}_0 = 0$.
In this case we have $\dot{V} + W_3 = \sigma_1(u_1 + \sigma_2) + \sigma_3$. For $\sigma_3$ we have $\sigma_3 \leq k_1 \left(\frac{x_1}{\pi_1}\right)\sin\left(\frac{x_1}{m\pi_1}\right)v_r(\gamma_1 - 1) \leq 0$.

Here we choose $u_1$ similar to case 2 except that $\bar{x}_0 = 0$. When $x_2 \geq 0$, we get that

$$\sigma_1 u_1 + \sigma_2 \leq k_1 \left(\frac{|x_2|}{\pi_1}\right)\left[v_{\min} - v_r \cos\left(\frac{x_1}{m\pi_1}\right)\right]$$
$$+ \gamma_2 k_1 \left(\frac{|x_2|}{\pi_1}\right)[v_r \cos\left(\frac{x_1}{m\pi_1}\right) - v_{\min}]$$
$$= (\gamma_2 - 1)k_1 \left(\frac{|x_2|}{\pi_1}\right)\left[v_r \cos\left(\frac{x_1}{m\pi_1}\right) - v_{\min}\right],$$

which is nonpositive since $0 < \gamma_2 < 1$ and $m > 1/\cos^{-1}(v_{\min}/(v_{\min} + \epsilon_v))$.

When $x_2 < 0$, we get that

$$\sigma_1 u_1 + \sigma_2 \leq k_1 \left(-\frac{|x_2|}{\pi_1}\right)\epsilon_v + \gamma_2 k_1 \left(\frac{|x_2|}{\pi_1}\right)\epsilon_v$$
$$\leq (\gamma_2 - 1)k_1 \left(\frac{|x_2|}{\pi_1}\right)\epsilon_v,$$

which is also nonpositive. ∎

It is straightforward to show that $M_1$ and $M_2$ in Eqs. (19) and (20) are bounded as $|\alpha|$ approaches both 0 and $1/M_0$. Therefore $M_1$ and $M_2$ are finite and can be found by straightforward optimization techniques.

Theorem 4 demonstrates that $V$ is a valid CLF for system (10) under saturation constraints (9). Note that a very conservative upper bound is found for $m$ in each case for simplicity of the proof. In reality, $m$ can be much smaller than the upper bound specified above. Also note that all of the parameters can be computed numerically off-line. The resulting controller will be computationally simple.

## IV. NONLINEAR TRACKING CONTROL BASED ON CLF

With the CLF given in Theorem 4, our goal in this section is to find a family of feasible tracking control laws based on this CLF.

Following the notation introduced in the proof of Theorem 4, we get that $\dot{V} + W_3 = \lambda_0 u_0 + \lambda_1 u_1 - \bar{\lambda}$, where

$\lambda_0 \triangleq \frac{\bar{x}_0}{\pi_2}\left(m - \frac{x_2}{\pi_2}\right)$, $\lambda_1 \triangleq \sigma_1$, and $\bar{\lambda} \triangleq -\sigma_2 - \sigma_3 - \sigma_4$. Consider the line defined by

$$\lambda_0 u_0 + \lambda_1 u_1 = \bar{\lambda}, \tag{22}$$

which separates the control space into two halves, where the half plane $\lambda_0 u_0 + \lambda_1 u_1 \leq \bar{\lambda}$ represents unconstrained control values that ensure that $\dot{V} \leq -W_3(x)$. The input constraints (9) produce a time-varying rectangle in the $u_0$–$u_1$ plane. Theorem 4, guarantees a nonempty intersection between the half plane $\lambda_0 u_0 + \lambda_1 u_1 \leq \bar{\lambda}$ and the input constraints (9). We call this nonempty intersection the "feasible control set" and denote it by $\mathcal{F}(t, x)$.

We have the following theorem.

*Theorem 5:* If the time-varying feedback control law $k(t, x)$ satisfies $k(t, 0) = 0$, $k(t, x) \in \mathcal{F}(t, x)$, $\forall x \neq 0$, and $k(t, x)$ is locally Lipschitz in $x$ and piecewise continuous in $t$, $\forall x \neq 0$ and $\forall t \geq 0$, then this control solves the tracking problem with input constraints, that is, $|x_r - x| + |y_r - y| + |\psi_r - \psi| \rightarrow 0$ as $t \rightarrow \infty$.

*Proof:* Straightforward using standard Lyapunov stability theory for time-varying systems. ∎

There are an infinite number of possibilities for selecting a feedback strategy that satisfies Theorem 5. In this paper we will investigate the performance of a simple saturation control.

*Lemma 6:* If

$$u_0 = \begin{cases} -\eta_0 \bar{x}_0, & |\eta_0 \bar{x}_0| \leq \epsilon_\omega \\ -\text{sign}(\bar{x}_0)\epsilon_\omega, & |\eta_0 \bar{x}_0| > \epsilon_\omega \end{cases} \tag{23}$$

$$u_1 = \begin{cases} \underline{v}, & -\eta_1 x_2 < \underline{v} \\ -\eta_1 x_2, & \underline{v} \leq -\eta_1 x_2 \leq \bar{v} \\ \bar{v}, & -\eta_1 x_2 > \bar{v} \end{cases} \tag{24}$$

then $k_{sat}(t, x) = [u_0, u_1]^T$ satisfies the conditions of Theorem 5 for sufficiently large $\eta_0 > 0$ and $\eta_1 > 0$.

*Proof:* The proof follows a similar line as that in Theorem 4 and is omitted here for space limitations. ∎

In Lemma 6 we used a simple control law that stays in the feasible control set. Other continuous saturation functions like atan, tanh are also possible as long as they stay in the feasible control set. In the case of $v_r$ and $\omega_r$ being uniformly continuous, it is also possible to use geometrical strategies to find feasible control laws (e.g. choose the geometrical center of the feasible control set $\mathcal{F}(t, x)$ as feasible controls).

One advantage of the CLF-based approach used in this paper is that it only requires $v_r$ and $\omega_r$ to be piecewise continuous instead of being uniformly continuous, which results in wider potential applications than other approaches which requires uniform continuity. Note that if we go back to the original system defined by (3), we can see that $v^c = u_1 + v_r \cos(x_0)$ and $\omega^c = \omega_r - u_0$, which is piecewise continuous in $t$ since $v_r$ and $\omega_r$ are piecewise continuous in $t$. The other advantage is that it provides the possibility to use other advanced strategies to choose feasible controls from $\mathcal{F}(t, x)$.

For example, at each time $t$, a feasible control may be generated from $\mathcal{F}(t, x)$ while optimizing some performance index function or minimizing some cost function at the same time, which introduces more flexibility and benefits to the tracking control problem than specifying a fixed control law in advance. In addition, it is also possible to propose a suboptimal controller from $\mathcal{F}(t, x)$ based on the combination of model predictive techniques and the tracking CLF.

## V. SIMULATION RESULTS

In this section, we simulate a scenario where a small fixed wing UAV is assigned to transition through several known targets in the presence of dynamic threats. The overall system architecture consists of Waypoint Path Planner (WPP), Dynamic Trajectory Smoother (DTS), Trajectory Tracker (TT), Low-level Autopilot, and UAV.

The design of the WPP and DTS are described in [11] and [8], respectively. The WPP produces waypoint paths that change in accordance with the dynamic threat environment. The DTS smoothes through these waypoints and produces a feasible time-parameterized trajectory that satisfies Eq. (4) and the constraints for reference inputs.

The parameters used in this paper are given in Table I.

| Parameter | Value | Parameter | Value |
|---|---|---|---|
| $v_{min}$ | 1.0 (m/s) | $v_{max}$ | 2.0 (m/s) |
| $\omega_{max}$ | 1.7 (rad/s) | $\epsilon_1$ | 0.2 (m/s) |
| $\epsilon_2$ | 0.2 (rad/s) | $v_r$ | $\in [1.2, 1.8]$ (m/s) |
| $\omega_r$ | $\in [-1.5, 1.5]$ (rad/s) | $\alpha_\psi$ | 5 |
| $\alpha_v$ | 50 | $m$ | 100 |
| $k_1$ | 2 | $\gamma_0, \gamma_1, \gamma_2$ | 0.5 |
| $\eta_0$ | 10 | $\eta_1$ | 10 |

TABLE I

PARAMETER VALUES USED IN SIMULATION.

Figure 1 shows the problem scenario. The dots are threat locations to be avoided. The waypoint path planner described in [11] generates the waypoint path which is shown in green. The dynamic trajectory smoother described in [8] generates the reference trajectory, which is shown in red. The actual trajectory is shown in blue.

The trajectory tracking errors for position and heading angle are plotted in Figure 2. We can see that the tracking error for heading angle converges faster than that for $x$ and $y$ coordinate, which is due to the weighting factor $m$ in the definition of $\bar{x}_0$.

The reference and commanded control inputs are plotted in Figure 3. Obviously, $v_r$ and $\omega_r$ are only piecewise continuous instead of uniformly continuous. The reference control inputs generated by the trajectory generator satisfy their constraints respectively, that is, $v_r \in [1.2, 1.8]$ m/s and $\omega_r \in [-1.5, 1.5]$ rad/s. The commanded control inputs $v^c$ and $\omega^c$ are within the range $[1, 2]$ m/s and $[-1.7, 1.7]$ rad/s respectively, which satisfies the input constraints. The original heading rate plot
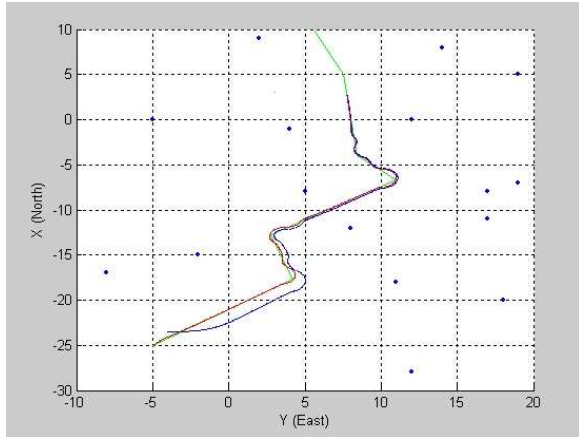
Fig. 1. The simulation scenario: waypoint path (green), smoothed reference trajectory (red), and actual trajectory (blue).

$\omega^c$ is somewhat chattering due to the abrupt change of the reference heading rate $\omega_r$, discrete implementation of the system with a sample rate of 20 Hz, and the high gain $m$ in the definition of $\bar{x}_0$. The chattering phenomenon is overcome by adding a low pass filter after the control signal $\omega^c$.
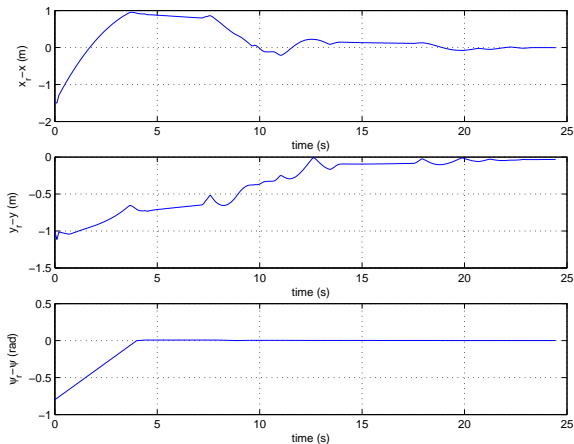


Fig. 2. The trajectory tracking errors expressed in the inertial frame.

## VI. CONCLUSION

A tracking CLF for a UAV kinematic models with input constraints is derived. Based on this CLF, a feasible control set is formed. This feasible control set facilitates the generation of a variety of feasible control strategies that not only guarantee accurate tracking but also optimize auxiliary performance functions. A simple saturation control strategy generated from the feasible control set was used and applied to a non-trivial simulation scenario.
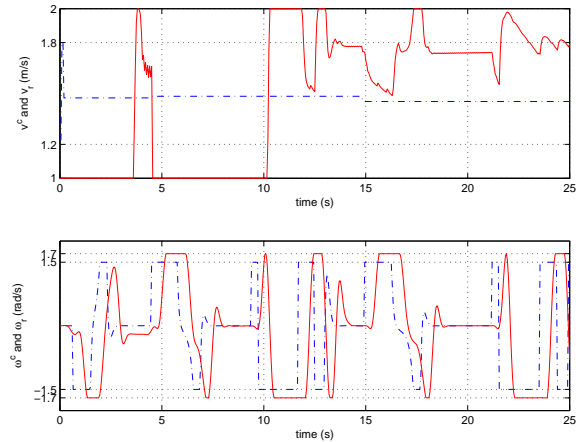
### Acknowledgments

Fig. 3. The commanded control inputs $v^c$ and $\omega^c$ (solid line) and reference control inputs $v_r$ and $\omega_r$ (dashdot line).

## VII. REFERENCES

[1] R. W. Brockett, "Asymptotic stability and feedback stabilization," in *Differential Geometric Control Theory* (R. S. Millman and H. J. Sussmann, eds.), pp. 181–191, Birkhaüser, 1983.

[2] J.-M. Yang and J.-H. Kim, "Sliding mode motion control of nonholonomic mobile robots," *IEEE Control Systems Magazine*, vol. 19, pp. 15–23, April 1999.

[3] Z.-P. Jiang, E. Lefeber, and H. Nijmeijer, "Saturated stabilization and track control of a nonholonomic mobile robot," *Systems and Control Letters*, vol. 42, pp. 327–332, 2001.

[4] T.-C. Lee, K.-T. Song, C.-H. Lee, and C.-C. Teng, "Tracking control of unicycle-modeled mobile robots using a saturation feedback controller," *IEEE Transactions on Control Systems Technology*, vol. 9, pp. 305–318, March 2001.

[5] Z. Artstein, "Stabilization with relaxed controls," *Nonlinear Analysis, Theory, Methods, and Applications*, vol. 7, no. 11, pp. 1163–1173, 1983.

[6] E. D. Sontag, "A Lyapunov-like characterization of asymptotic controllability," *SIAM Journal on Control and Optimization*, vol. 21, pp. 462–471, May 1983.

[7] J. W. Curtis and R. W. Beard, "Satisficing: A new approach to constructive nonlinear control," *IEEE Transactions on Automatic Control*, (in review).

[8] E. P. Anderson and R. W. Beard, "An algorithmic implementation of constrained extremal control for UAVs," in *Proceedings of the AIAA Guidance, Navigation, and Control Conference*, (Monterey, CA), August 2002. Paper No. AIAA-2002-4470.

[9] A. W. Proud, M. Pachter, and J. J. D'Azzo, "Close formation flight control," in *Proceedings of the AIAA Guidance, Navigation, and Control Conference*, (Portland, OR), pp. 1231–1246, August 1999. Paper No. AIAA-99-4207.

[10] Y. J. Kanayama, Y. Kimura, F. Miyazaki, and T. Noguchi, "A stable tracking control method for an autonomous mobile robot," in *Proceedings of the IEEE International Conference on Robotics and Automation*, pp. 384–389, 1990.

[11] R. W. Beard, T. W. McLain, M. Goodrich, and E. P. Anderson, "Coordinated target assignment and intercept for unmanned air vehicles," *IEEE Transactions on Robotics and Automation*, vol. 18, pp. 911–922, December 2002.